



HAL
open science

Clockwise rotation of the Brahmaputra Valley relative to India: Tectonic convergence in the eastern Himalaya, Naga Hills, and Shillong Plateau

Philippe Vernant, R. Bilham, W. Szeliga, D. Drupka, S. Kalita, A. K. Bhattacharyya, V. K. Gaur, P. Pelgay, Rodolphe Cattin, Theo Berthet

► To cite this version:

Philippe Vernant, R. Bilham, W. Szeliga, D. Drupka, S. Kalita, et al.. Clockwise rotation of the Brahmaputra Valley relative to India: Tectonic convergence in the eastern Himalaya, Naga Hills, and Shillong Plateau. *Journal of Geophysical Research*, 2014, 119 (8), pp.6558-6571. 10.1002/2014JB011196 . hal-01115084

HAL Id: hal-01115084

<https://hal.science/hal-01115084>

Submitted on 11 May 2021

HAL is a multi-disciplinary open access archive for the deposit and dissemination of scientific research documents, whether they are published or not. The documents may come from teaching and research institutions in France or abroad, or from public or private research centers.

L'archive ouverte pluridisciplinaire **HAL**, est destinée au dépôt et à la diffusion de documents scientifiques de niveau recherche, publiés ou non, émanant des établissements d'enseignement et de recherche français ou étrangers, des laboratoires publics ou privés.

RESEARCH ARTICLE

10.1002/2014JB011196

Key Points:

- New GPS velocity field in eastern Himalaya
- Shillong Plateau is independent from India
- Strain accumulated since the last earthquake is sufficient for a $M > 8$ earthquake

Supporting Information:

- Readme
- Text S1
- Table S1

Correspondence to:

P. Vernant,
pvernant@um2.fr

Citation:

Vernant, P., R. Bilham, W. Szeliga, D. Drupka, S. Kalita, A. K. Bhattacharyya, V. K. Gaur, P. Pelgay, R. Cattin, and T. Berthet (2014), Clockwise rotation of the Brahmaputra Valley relative to India: Tectonic convergence in the eastern Himalaya, Naga Hills, and Shillong Plateau, *J. Geophys. Res. Solid Earth*, 119, 6558–6571, doi:10.1002/2014JB011196.

Received 14 APR 2014

Accepted 16 JUL 2014

Accepted article online 22 JUL 2014

Published online 6 AUG 2014

Clockwise rotation of the Brahmaputra Valley relative to India: Tectonic convergence in the eastern Himalaya, Naga Hills, and Shillong Plateau

P. Vernant¹, R. Bilham², W. Szeliga³, D. Drupka⁴, S. Kalita⁵, A. K. Bhattacharyya⁶, V. K. Gaur⁷, P. Pelgay⁴, R. Cattin¹, and T. Berthet¹

¹Géosciences Montpellier, Université Montpellier II, Montpellier, France, ²Geological Sciences and CIRES, University of Colorado Boulder, Boulder, Colorado, USA, ³Department of Geological Sciences, Central Washington University, Ellensburg, Washington, USA, ⁴Seismology and Geophysics Division, Department of Geology and Mines, Thimphu, Bhutan, ⁵Department of Environmental Sciences, Gauhati University, Assam, India, ⁶Tezpur University, Tezpur, India, ⁷CSIR Centre for Mathematical Modelling and Computer Simulation, Bangalore, India

Abstract GPS data reveal that the Brahmaputra Valley has broken from the Indian Plate and rotates clockwise relative to India about a point a few hundred kilometers west of the Shillong Plateau. The GPS velocity vectors define two distinct blocks separated by the Kopili fault upon which 2–3 mm/yr of dextral slip is observed: the Shillong block between longitudes 89 and 93°E rotating clockwise at 1.15°/Myr and the Assam block from 93.5°E to 97°E rotating at $\approx 1.13^\circ/\text{Myr}$. These two blocks are more than 120 km wide in a north-south sense, but they extend locally a similar distance beneath the Himalaya and Tibet. A result of these rotations is that convergence across the Himalaya east of Sikkim decreases in velocity eastward from 18 to ≈ 12 mm/yr and convergence between the Shillong Plateau and Bangladesh across the Dauki fault increases from 3 mm/yr in the west to > 8 mm/yr in the east. This fast convergence rate is inconsistent with inferred geological uplift rates on the plateau (if a 45°N dip is assumed for the Dauki fault) unless clockwise rotation of the Shillong block has increased substantially in the past 4–8 Myr. Such acceleration is consistent with the reported recent slowing in the convergence rate across the Bhutan Himalaya. The current slip potential near Bhutan, based on present-day convergence rates and assuming no great earthquake since 1713 A.D., is now ~ 5.4 m, similar to the slip reported from alluvial terraces that offsets across the Main Himalayan Thrust and sufficient to sustain a $M_w \geq 8.0$ earthquake in this area.

1. Introduction

The Himalayan arc (Figure 1) defined by the 3.5 km elevation contour follows an almost perfect small circle between 77° and 89° with radius of 1623 km centered at 42.10°N, 90.72°E [Seeber and Gornitz, 1983; Bendick and Bilham, 2001]. In the west, the Pir Pinjal range departs as a tangent from the small circle at $\approx 78^\circ\text{E}$ near the rupture zone of the 1905 Kangra rupture zone, and in the east, the 3.5 km contour mountains strike N70°E toward the eastern syntaxis as a chord that diverges near 92°E. Between these longitudes, the Indian Plate converges with the Tibetan Plateau at rates of 16–18 mm/yr. To the west, velocities slow to 12 mm/yr [Schiffman et al., 2013]. East of the 92° convergence velocities between the Tibetan Plateau and the Indian Plate rises to 31 mm/yr [Burgess et al., 2012]. The significance of the 3.5 km contour in the central Himalaya is that it approximates the location of the locking line north of which, at depths below ≈ 18 km, the Indian Plate is inferred to slide aseismically northward beneath the Himalaya [Bollinger et al., 2004]. South of the locking line, a cloud of microseismicity signifies the development and partial release of strain resulting from stress loading associated with Himalayan convergence [Bollinger et al., 2004]. In the central Himalaya, the correspondence between the 3.5 km contour and the microseismicity is striking since it follows minor erosional embayments in the mountains. Instrumentally located epicenters of moderate and great earthquakes follow the southern edge of the locking line [Ni and Barazangi, 1984]. If one uses the 3.5 km contour as a proxy for the northern edge of the décollement ruptured by great Himalayan earthquakes, for much of the Himalaya, the width of décollement defined by the radial separation between the locking line and the MFT (Main Frontal Fault) is 100–110 km (Figure 1). In Sikkim and Bhutan, however, five ridges with elevations locally exceeding 3.5 km extend southward

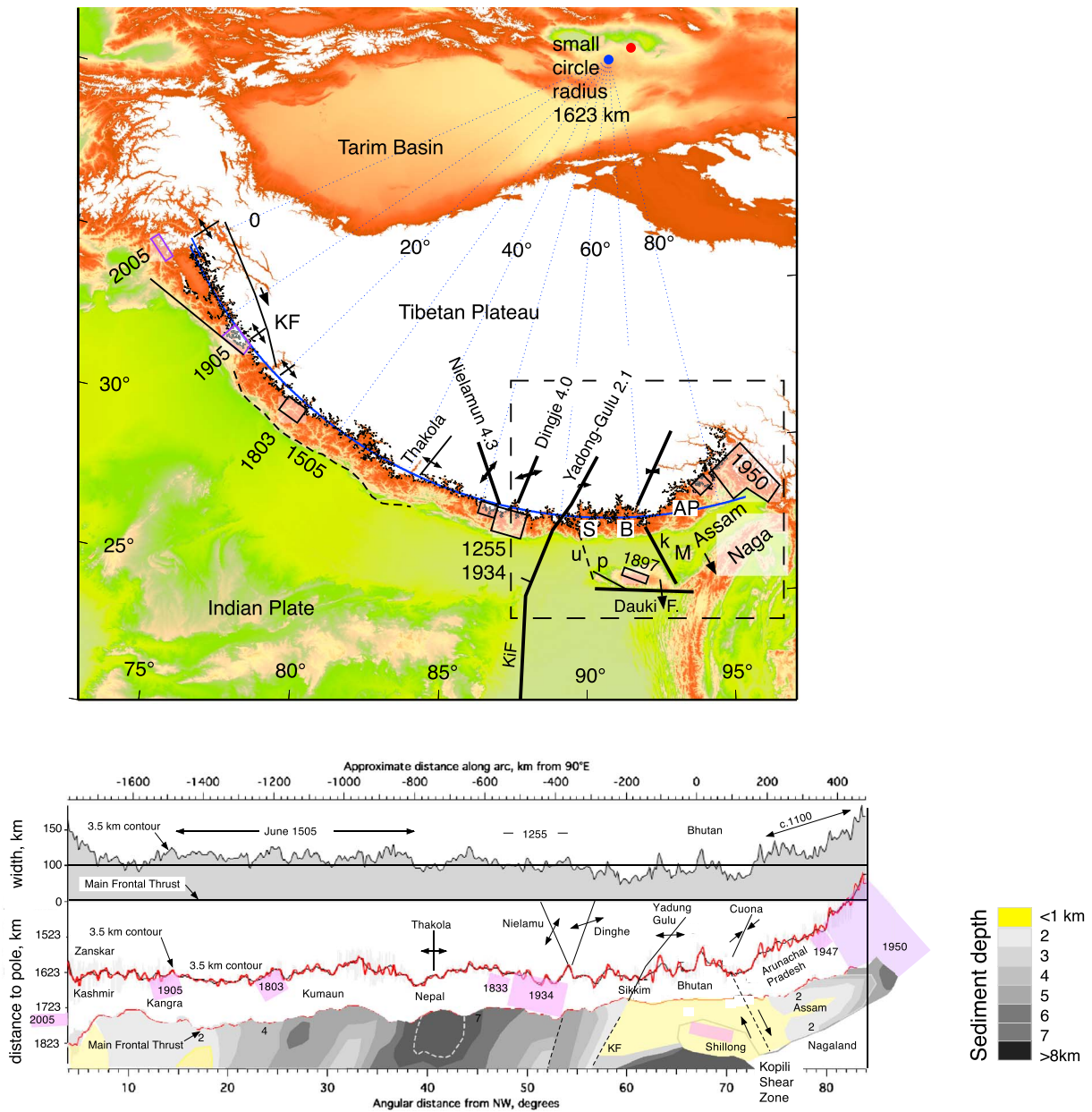


Figure 1. (a) Small circle fit to Himalaya showing pole and radius used in Figure 1b. West of the 1905 earthquake the Himalayan décollement broadens to include the Pir Pinjal [Schiffman *et al.*, 2013]. East of Bhutan, the Himalaya no longer follows a small circle (black arc) defined by elevations greater than 3.5 km (shaded white), the Tibetan Plateau is broken by pronounced rift zones, and no prominent foredeep lies south of Bhutan. Rupture zones of major earthquakes are indicated with dates. S = Sikkim, B = Bhutan, AP = Arunachal Pradesh, KF = Karakoram Fault, p = Dapsi Fault, k = inferred Kopili fault, KIF = Kishanganj Fault, u = approximate location of inferred Dhubri fault, and M = Mikir Hills. Dates indicate the rupture zones of historical earthquakes. Inset shows the location of Figure 3. (b) A cylindrical projection of the Himalaya. The top row shows the width of the décollement plotted as a function of distance from the Main Frontal Thrust showing the along-arc variation in the width of the décollement and dates of inferred rupture zones (violet). Note that the width of the décollement averages 110 km for the 1505 rupture and averages less than 90 km near Sikkim and Bhutan. The bottom row shows the northern and southern limits of the Himalayan décollement as a function of distance from the small circle pole and sediment depth in the flexural fore-arc basin [Dasgupta *et al.*, 2000] and its abrupt shallowing between Bhutan and the Shillong Plateau. Prominent rift zones are indicated by Gan *et al.* [2007].

from the edge of the Tibetan Plateau to approach within 30 km of the MFT, significantly closer than elsewhere in the Himalaya.

These remarkable changes in the geometry of the Himalayan arc near Bhutan are accompanied by a segmented block like behavior of the southern Tibetan Plateau [Chen *et al.*, 2004; Thatcher, 2007; Meade, 2007; Ismail-Zadeh *et al.*, 2007]. To the west of Bhutan, the blocks are separated by sinistral rift zones (green lines in

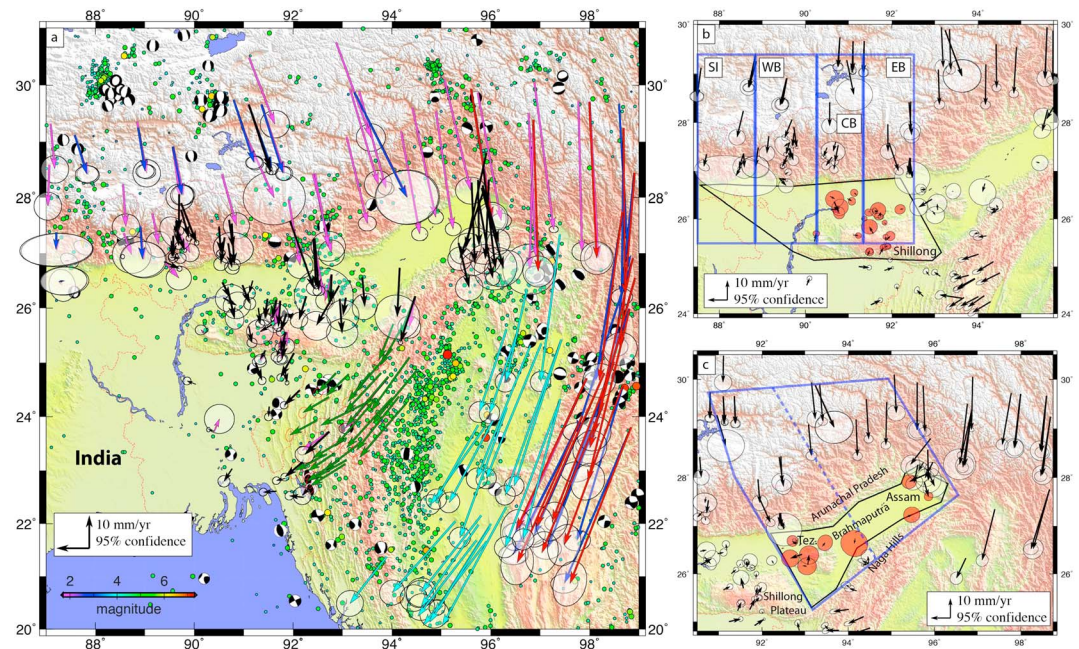


Figure 2. GPS vectors and seismicity NW India and Southern Tibet. (a) Indian Plate fixed. (b) Shillong Plateau fixed. (c) Assam block fixed. The blue rectangles indicate the regions subject to velocity field analysis (Table 2). The colored arrows indicate the GPS vectors derived from different sources (see text). Tez = Tezpur.

Figure 2) widening at ≈ 3 mm/yr [Armijo *et al.*, 1986; Zhang *et al.*, 2004; Gan *et al.*, 2007]. North of eastern Bhutan, a weakly expressed sinistral shear zone (blue line in Figure 2) converges at less than 1 mm/yr [Gan *et al.*, 2007].

The tectonic architecture of the Indian Craton, south of Bhutan, is no less unique. Whereas the Brahmaputra/Ganges foredeep attains depths of 4 km, some 250 km to the east and west of Bhutan's frontiers (Figure 1b), geophysical data indicate that it may be less than 1 km thick south of Bhutan [Dasgupta *et al.*, 2000; Verma and Mukhopadhyay, 1977]. Observed shaking intensities in the 1934 and 1897 earthquakes were subdued in the shallow sediments south of Bhutan but amplified by the thick sediments in the river plains, SE and SW of Bhutan [Hough and Bilham, 2008]. Archean basement rarely approaches closer than 200 km to the frontal thrusts of the Himalaya, but south of Bhutan, and near Tezpur, the Brahmaputra passes between rock inselbergs that surface within 35 km of the MFT. The replacement of a prominent flexural foredeep by a shallow crystalline platform here [Clark and Bilham, 2008; Dasgupta and Nandy, 1982; Dasgupta *et al.*, 1987] suggests that the mechanisms that support the rise of Shillong Plateau are related. This lateral variation is also consistent with the west-to-east decrease in flexural wavelength described by Jordan and Watts [2005], Berthet *et al.* [2013], and Hammer *et al.* [2013]. The plateau is bounded by the Dauki thrust fault to the south and by the buried dextral Kopili shear zone [Kayal *et al.*, 2010] to the east (Figure 4). Focal mechanisms suggest strike-slip faulting on the inferred Dhubri fault to the west (Figure 4), whose southward continuation is associated by Steckler *et al.* [2008] with Indo-Burman convergence processes. It is not clear how the Dhubri fault continues northward beneath the Brahmaputra river, west of the crystalline inselbergs through which the river passes. We show below that this region lies near the pole of rotation between the Shillong block and the Indian Plate.

The uplift of the northern edge of the Shillong Plateau of ≈ 10 m occurred in the 1897 $M_w = 8.1$ earthquake [Oldham, 1899; Bilham and England, 2001]. The fault plane was 110 km long, with ESE strike, dipping south between 9 and 35 km depth, and although no surface slip occurred, evidence for subsurface reverse slip is preserved in steepened drainages north of the crest of the plateau [Clark and Bilham, 2008]. Seismicity beneath Shillong extends to depths exceeding 50 km [Chen and Molnar, 1990; Kayal *et al.*, 2006] and although focal mechanisms have been used to interpret stress azimuths [Angelier and Baruah, 2009], as yet no simple subsurface geometry has been inferred from the distribution of microseismicity. Six $M_w \geq 7$ earthquakes

Table 1. Rotation Poles for the Plates and Blocks NE India Determined in This Study (ts) and *Gahalaut and Gahalaut* [2007] Study (GG)

Block Pairs	Longitude (°E)	Latitude (°N)	Rotation (°/Myr)	Rotation Uncertainty	Major Axis	Minor Axis	Major Axis (az)	Study
Shillong/India	88.78	26.43	−1.149	0.036	0.10	0.06	−178.7	ts
Assam/India	87.77	26.76	−1.130	0.190	1.05	0.11	−177.9	ts
Assam/Shillong	129.53	5.93	0.027	0.147	110.15	5.56	145.0	ts
BhutanH/Shillong	80.63	28.87	−0.969	0.061	0.83	0.17	178.7	ts
ArunachalH/Assam	81.98	28.50	−0.986	0.195	2.68	0.21	173.2	ts
SikkimH/India	63.10	26.71	−0.377	0.087	7.62	0.55	−168.5	ts
SikkimH/Shillong	100.14	24.80	0.816	0.099	1.96	0.28	−22.8	ts
Assam/NagaHills	103.22	35.88	0.125	0.193	27.33	1.79	−137.0	ts
India/Burma	89.17	27.74	1.251	0.052	0.31	0.08	−35.8	ts
India/Burma	82	27	0.845		1	1	0	GG

occurred in the region surrounding the Shillong Plateau between 1838 and 1948, more than in the entire eastern Himalaya in a similar period [Ambraseys and Douglas, 2004]. With the exception of secondary surface faults in the 1897 earthquake [Oldham, 1899], no surface faulting has been reported from any of these major earthquakes.

2. GPS Velocities in NE India

We supplemented published GPS data from Nepal, Sikkim, Assam, Meghalaya, Tibet, and Bangladesh [Banerjee et al., 2008; Zhang et al., 2004; Shen et al., 2005; Ader et al., 2012; Maurin et al., 2010; Gahalaut et al., 2013], with new data from the Kingdom of Bhutan acquired in 2001, 2003, and 2012 (see the supporting information). Points in Bhutan were placed on rock outcrops where possible but, in some cases, on large boulders or on structures. Points were occupied for at least 48 h in the 2003 and 2006 surveys and at least 24 h in 2012. Some of the monuments were not recovered in 2012. Continuous measurements were obtained at Thimphu and Phuentsholing for more than 3 years until interrupted by local construction activities. We used Trimble 5700, NetRS and NetR9 receivers with Zephyr antennas for the campaign points, and NetRS receivers and choke ring antennas for the fixed sites (Table 1). The data were processed in the U.S. and in France with consistent results using GAMIT and GLOBK software [Herring et al., 2009]. We corrected the data for the inferred coseismic displacements of $M_w > 6$ earthquakes in 2006 (Bhutan) and 2011 (Nepal) using the Harvard centroid moment tensor solutions, but the adjustments do not substantially alter our interpretation. Further analysis details are to be found in the supporting information.

In an India-fixed frame, convergence rates between southern Tibet and India increase eastward across the Himalaya from 18 mm/yr in eastern Nepal [Ader et al., 2012] to 31 mm/yr in eastern Assam (Figure 2a) [Burgess et al., 2012]. We note however that points in the northern Shillong Plateau and in the Brahmaputra Valley, south of Bhutan, move little relative to each other, and we consider that they lie upon an inferred rigid block. If we assume that the mean velocity of these points determines the translation and rotation of this rigid block, we can compute its pole and rotational velocity relative to India (Figure 3). We find that it rotates clockwise about a Euler pole near southern Sikkim. Similarly, we find that points in the Brahmaputra Valley to the east of the Kopili fault move little relative to each other, but their mean position (on an inferred Assam block) rotates clockwise relative to India about a pole close to the Shillong/India pole. The effect of clockwise rotation of these two inferred blocks is that convergence rates between the Brahmaputra Valley with southern Tibet east of Sikkim decrease eastward (Figure 2b). Minimizing the relative motion between selected GPS points in the Brahmaputra Valley in a least squares sense yields rotation rates of 1.15°/Myr for the Shillong block and 1.13°/Myr for the Assam block (Figure 2c), with dextral shear (≤ 3 mm/yr) across the Kopili shear zone. The sparsity of GPS data within the sediments of the Brahmaputra Valley provides weaker constraints on the rotation rate of the Assam block than that for the Shillong block.

The above calculations to determine relative rotation poles between India and the inferred Shillong and Assam blocks were undertaken by minimizing velocities in a least squares sense and searching for the three parameters that define a pole and angular velocity for selected points between the inferred blocks and the rigid Indian Plate. This procedure works well if the selected blocks act as rigid plates. It works less well where the surface velocity field near the edges of blocks may be influenced by elastic velocity fields resulting from relative slip at depth. Hence, in our search for rotation poles and in forward models to

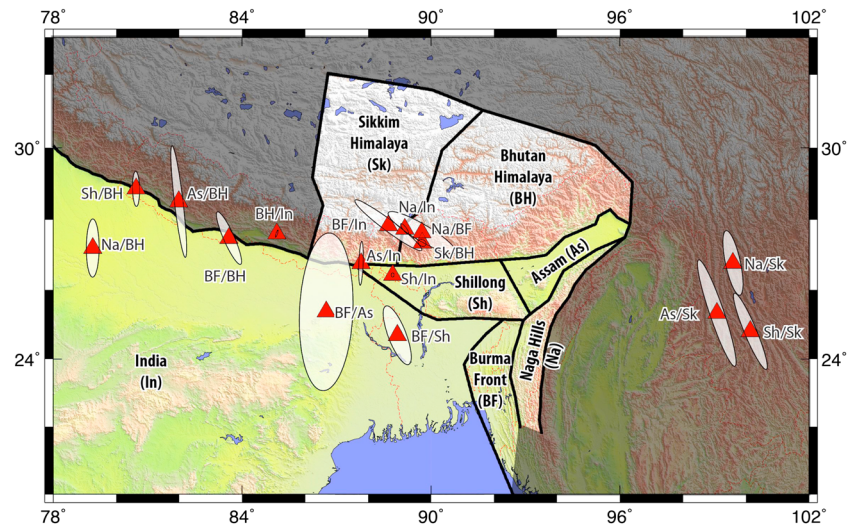


Figure 3. Blocks and their relative poles of rotation from Table 1. The northern extents of the blocks are conjectural; e.g., the Shillong and Assam blocks lie an unknown distance beneath the Himalaya and southern Tibet.

determine depth and velocity of Himalayan convergence (supporting information), we discarded data from points close to the southern edge of the Shillong Plateau, where the Dauki fault converges with the Indian Plate in Bangladesh, and from the eastern end of the Brahmaputra Valley, where possible elastic effects may result from shear strain.

As an independent test of our calculations, we employed DEFNODE [McCaffrey, 2002] to estimate rotation of the Himalaya relative to southern Tibet and to the northern Indo-Burman range [Gahalaut and Gahalaut, 2007]. DEFNODE solves both for block rotations on a sphere as above, but in addition solves for elastic strain accumulation on block-bounding faults. Bounding velocities are calculated, following the formulation of Okada [1985], by minimizing the GPS residual motions within the blocks in a least squares sense (Figure 3). In this model, no permanent deformation of the blocks or slip on isolated faults is permitted (i.e., all faults used in the model must be associated with a block boundary). Our goal is to determine fault slip rates by decomposing relative block motions on block boundaries into fault parallel (strike slip and positive left-lateral) and fault-normal motions (normal and thrust and positive compression). The rates so obtained provide an upper bound, since in this model, all the deformation is focused on the block boundaries (Figure 4a). As a consequence, the poles and angular velocities derived from DEFNODE differ slightly from those derived by the forward modeling method described earlier, but they are not necessarily more reliable, since they treat data derived from near the edges of the blocks as a contribution to block boundary deformation objectively, without geological constraints. In our forward models, we exclude data suspected (from independent geological information) to be near a subsurface source of strain. Because DEFNODE is able to solve simultaneously for subsurface deformation near block boundaries, and translation and rotation of blocks, we may examine conjectural blocks, whether or not their boundaries are clearly defined by independent geological constraints (Figure 3).

For example, the two blocks north of the MFT in Figure 3 include the elastic velocity fields resulting from the interaction between the northward moving and descending Indian Plate below ≈ 20 km (here represented by the inferred Shillong and Assam blocks) and the overriding Tibetan Plateau and Himalaya. Clearly, the southern boundaries of these “blocks” and the northern boundary of the Shillong or Assam blocks, though depicted in Figure 3 as following the MFT, instead, overlap each other for more than 100 km. They adhered to each other on the locked Himalayan décollement between great earthquakes, but north of the locked décollement, they are free to move relative to each other along a subhorizontal creeping surface. Thus, the blocks in our model are stacked upon one another and become distinct entities only south of the frontal thrusts. The MFT has a dip of $\approx 8^\circ$ N, the Dauki fault a dip of 60° N, and the thrusts, west of the Indo-Burman ranges and in the Naga hills, are assigned a dip of 30° E. All the other faults are assumed to be subvertical. The DEFNODE and forward models derive independent estimates of convergence at the locking north of which

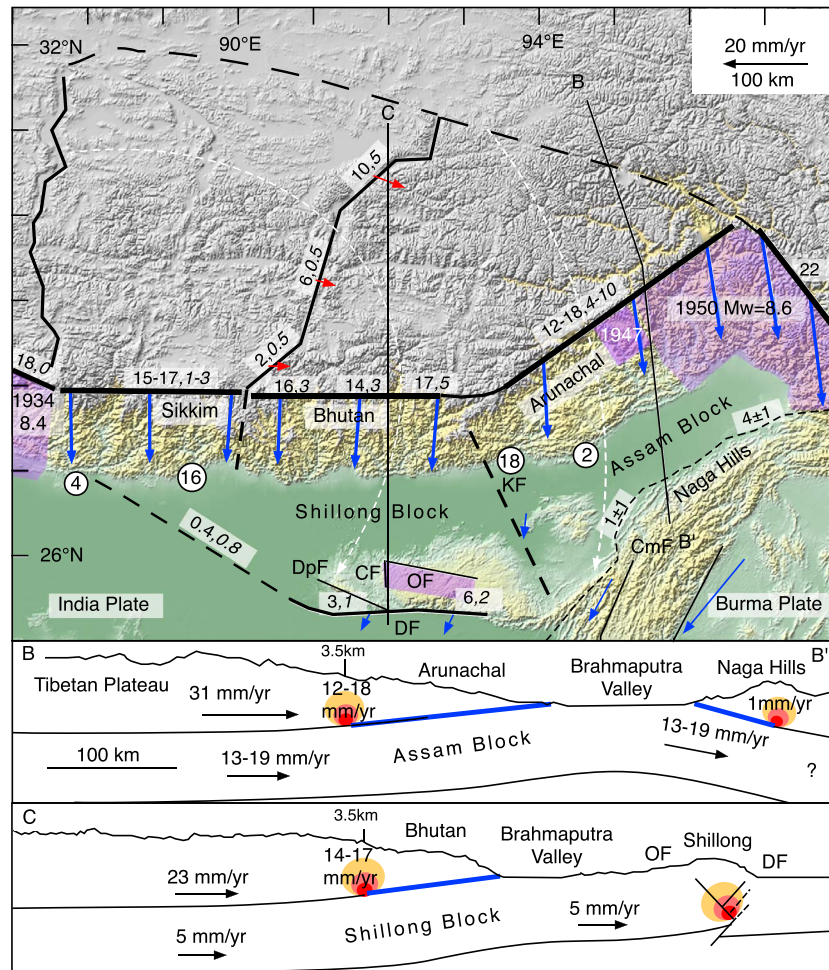


Figure 4. Structural relationships between the Brahmaputra Valley blocks and contiguous regions. The violet areas indicate the inferred rupture zones of recent major earthquakes. The circled numbers are the paleoseismic slip shown in meter [Kumar *et al.*, 2006, 2010; Nakata, 1972, 1989; Jayangondaperumal *et al.*, 2011]. The area in grey lies above 3.5 km. The straight black lines are the approximate locking line with numerical convergence in mm/yr and dextral shear (*in italics*). The white dashed arcs indicate the approximate trajectory of points on the Shillong and Assam blocks. The black dashed and solid lines show the block boundaries used in the models (the MFT follows the topographic break at the southern edge of the Himalaya). A range of calculated relative velocities are shown, where DEFNODE and analytical models differ. Faults indicated DpF Dapsi, CF Chedrang, OF Oldham, DF Dauki, CmfF Churachandpur-Mao, and KF Kopili. The schematic cross sections below the figure illustrate the locked décollements and velocities relative to the Indian Plate. The numbers on the strain accumulation areas indicate a range of inferred accumulation rates from DEFNODE and dislocation models presented in the supporting information.

creep mechanisms prevail. Differences between the numerical results are most evident where the GPS data are sparse. In such cases, we consider our forward models to be more reliable, since the data used in their derivation are selected based on geological (but admittedly subjective) considerations.

2.1. Rotation of the Shillong Block and Convergence With India

Previous estimates of convergence rate between the Shillong Plateau and the Indian Plate have been derived directly from geodetic data: 6 ± 6 mm/yr [Bilham and England, 2001], 4.3 ± 4.8 mm/yr [Jade *et al.*, 2007], and indirectly from exhumation rates assuming a northerly dip to the Dauki fault of $37\text{--}58^\circ$ at 91.5°E ($0.65\text{--}2.3$ mm/a [Biswas *et al.*, 2007]; $1\text{--}2.9$ mm/yr [Clark and Bilham, 2008]). Relative to the Indian Plate, the Shillong Plateau converges with the Indian Plate across the Dauki fault at rates that increase from ≈ 3 mm/yr in the west to ≈ 7 mm/yr in the east, with minor dextral shear. The elevation of the Shillong Plateau increases eastward, consistent with eastward increasing convergence rates; however, the long-term average vertical

Table 2. Locking Depths, Décollement Widths, and Convergence Velocities for the Eastern Himalaya (See Supporting Information for Synthetic/Observed Dislocation Models)

Segment	Longitude Range	Latitude	Convergence	Sinistral	Depth	Dip	Width	DEFNODE (mm/yr)	
		Lock (°N)	(mm/yr)	(mm/yr)	(km)	(°N)	(km)	North	Sinistral
Eastern Nepal	85–86°E	27.76	18 ± 1	0	19 ± 2	7 ± 2	100 ± 10	-	-
Sikkim	87.2–88.8°E	27.46	17 ± 1	3 ± 1	23 ± 9	5 ± 2	55–70	15	2
Western Bhutan	89–90°E	27.74	16.5 ± 1.5	2 ± 2	23 ± 5	7 ± 2	98 ± 10	17	1
Central Bhutan	90.4–91.4°E	27.65	15 ± 1.5	4 ± 2	23 ± 4	7 ± 2	80 ± 10	14	3
Eastern Bhutan	91.5–93°E	27.39	17.0 ± 1	-	14 ± 5	7 ± 5	60 ± 10	17	5
Western Assam	92–94°E	-	14 ± 1	-	±24	7 ± 3	>120	18	10
Arunachal	94–95°E	-	11.5 ± 1	4 ± 1	-	-	-	-	-
Eastern Assam	>95°E	-	14 ± 2	-	±10	-	-	-	-

^aDEFNODE estimates indicate both fault-normal and fault-parallel slip rates at midsegments of the block boundaries; *Karakhanyan et al.* [2013] suggest that ±1 mm/yr of uncertainty on the DEFNODE estimates is more realistic than the formal uncertainties, which are usually too optimistic. For some segments, insufficient data prevented the calculation of meaningful numerical solutions.

faulting rate of 0.7–1.4 mm/yr (derived by *Clark and Bilham* [2008] from geological exhumation rates) at 91.5°E is inconsistent with the present-day convergence rate of 6 ± 1 mm/yr, unless an unexpectedly low dip (<13°N) prevails for the Dauki fault. Based on our new GPS results, we argue below that the apparent discrepancy can be explained if the present rate of convergence across the Dauki fault is approximately 3 times faster than the average rate in the past 10 Myr.

The rotation pole between India and Shillong is approximately in line with the strike of the 1897 $M_w = 8.1$ Oldham fault earthquake [*Bilham and England*, 2001] and the Dapsi fault [*Kayal et al.*, 2006]. Thus, these two fault planes follow approximate radii from the pole of rotation and would be expected to exhibit pure convergence when they slip. A mean convergence rate across the subsurface Oldham fault of 5 mm/yr, given the pole and angular rotation between Shillong and India (Table 2), implies a renewal time for 16 m reverse slip earthquakes (≈10 m of contraction) of ≈2000 years. Occasional reverse slip on the subparallel Dapsi or Dauki faults would reduce the rate on the Dauki fault and extend the renewal time to more than 2000 years. *Morino et al.* [2011] infer a significant earthquake to have occurred in the sixteenth century on the western Dauki fault. Slip during this inferred earthquake is presently unknown, since their trench did not expose the primary rupture. The eastward doubling in convergence rate however implies a shorter recurrence interval for major earthquakes on the eastern Dauki fault or larger-slip events when they occur.

2.2. Himalayan Convergence

Present-day convergence in Bhutan averages to 14–17 mm/yr (Table 2 and the supporting information). In western Bhutan, where we have a sufficient density of GPS points to determine the decay in velocity southward across the décollement, the velocity field is similar to that observed elsewhere in the Himalaya; i.e., the data confirm a locking line north of which the Indian Plate creeps aseismically below the Tibetan Plateau, with no creep to its south on the Himalayan décollement. We conclude that Bhutan is not immune from great earthquakes. By assuming that creep is absent throughout the décollement (south of the locking line) from eastern Nepal to eastern Assam, we can determine the décollement width, locking depth, convergence velocity, and best fitting dislocations corresponding to regions where we may anticipate future earthquakes (Table 2 and the supporting information). In Sikkim, the décollement is anomalously narrow, and the data available show considerable scatter. *Mullick et al.* [2009] interpret these same data in terms of shear faulting south of the MFT.

The largest discrepancy between DEFNODE and independent dislocation solutions in our analyses occurs east of Bhutan. The central Arunachal Pradesh segment of the Himalaya has presently few GPS points and none that are suitable for determining the locking depth or its precise location. Elsewhere, we find a close correspondence between the 3.5 km contour and the locking line, and hence, we infer a 120–130 km wide décollement that exists here. From the two points in Tibet >80 km to the northwest of the locking line (Figure S5 in the supporting information), we surmise that a convergence velocity of 11.5 ± 1 mm/yr prevails with a sinistral shear velocity of 3–5 mm/yr. DEFNODE for the same segment however determines a convergence rate of 18 mm/yr and a sinistral shear rate of 10 mm/yr. The large difference between the two solutions is related to the scarcity of the sites in the region and how the block geometry is defined. *Burgess et al.* [2012]

determine a minimum Holocene convergence velocity from geological evidence at longitude $92^{\circ}40'$ of 23 ± 6.2 mm/yr, with a minimum shortening rate in the past 2 Myr of 13 mm/yr. Their minimum convergence rates are somewhat ($\approx 10\%$) faster than those we derive from our GPS estimates.

We note that the great width of the locked décollement in Arunachal Pradesh is accompanied by an attendant reduction in the average accretionary slope from 2.2° near Bhutan to 1.5° farther east. The gentle slope is suggestive of disequilibrium in the wedge angle of the Himalayan accretionary prism [Dahlen, 1990], suggesting that out-of-sequence thrust faulting near the locking line may currently be a preferred failure mode. The magnitude of the 1947 $M_w = 7.7$ earthquake in northern Arunachal [Chen and Molnar, 1977] was insufficiently large to rupture the entire décollement and may have occurred on an out-of-sequence thrust.

2.3. Convergence Between the Naga Hills and the Brahmaputra Valley

The poles of rotation of the Burma Plate and the Assam Valley relative to India (Table 2) indicate slow convergence in the Naga Hills. Using these rotation poles, we find that convergence increases from 1–2 mm/yr in the west, south of the Mikir Hills, to more than 5 mm/yr in the east. Our DEFNODE solution, however, incorporating data from the Indo-Burman ranges, prefers approximately uniform convergence of 3 mm/yr with negligible shear across the Naga Hills. Although these rates are slow, they are similar to those observed before the 2008 Wenchuan earthquake [Godard *et al.*, 2010] and are presumably responsible for a major earthquake in 1548 that is known from sparse historical data to have damaged cities near longitude 95° .

2.4. Great Earthquakes in the Eastern Himalaya

The recurrence rate of the $M_w < 7.5$ earthquakes is too low to account for the observed present-day convergence rate. At 1.4–1.8 m/century (Table 2), the $M_w = 7$ earthquakes could occur once per century at hundred kilometer intervals along the eastern Himalaya or roughly once every two decades in our area of study. The actual rate of the $M \approx 7$ earthquakes is one per century. Moreover, our analysis of velocity fields reveals no strainfields that are characteristic of creep south of the locking line. Consequently, we conclude that the slip deficit currently developing will be released by future great earthquakes with a slip of 5–20 m, as elsewhere in the Himalaya. Clues to the imminence of these future earthquakes, assuming that present-day deformation is similar in rate and style to historical deformation, are to be found in the timing of former great earthquakes in the Assam Himalaya. Where great earthquakes occur, but have not occurred for some considerable time, we may anticipate future great earthquakes sooner than in locations where they have occurred in the recent past. In the next three paragraphs, we summarize the current status of knowledge of historical earthquakes in Assam.

The written record in the Brahmaputra Valley prior to the nineteenth century is sparse. *Iyengar et al.* [1999] identify several damaging earthquakes in Assam that have been described in local histories, but these accounts are from single locations and few described damage that is readily interpreted in terms of shaking intensity: 1548 Garhgoan near the Naga Hills (26.7°N , 94.8°E), 1596 Gajala and 1663 Kajali near the Kopili Fault (26.3°N , 92.7°E), 1697 Sadiya near the main Himalayan Frontal thrust (27.8°N , 94.6°E), and circa 1714 Tinkhang (27.21°N , 95.02°E) near Garhgoan. The locations of these reported earthquakes are plotted on Figure 4, indexed by the year of their occurrence; however, although their retention in recorded histories suggests they were damaging, their magnitudes are unknown. One reason for the surviving record to remain ambiguous is that the normal measures of intensity are derived from the collapse of structures with different degrees of fragility. Indigenous construction in Assam uses wood or bamboo, and masonry structures were historically largely restricted to temples or palaces, in which the Brahmaputra Valley are now in states of extensive ruin. Many were repaired following the damage in the 1897 earthquake, and dates of pre-1897 collapse are routinely assigned to former earthquakes [e.g., *Gait*, 1906; *Banerji*, 1923], although few forensic excavations of undisturbed temples have been undertaken with a view to determining their dates of collapse. *Choudhury* [1985] concludes from stylistic features that several medieval stone temples may have been assembled using materials from former earthquake ruins.

Much of Bhutan's historical record was lost during the 1897 Shillong earthquake and in accidental fires in Bhutan in the nineteenth century [White, 1909]. However, surviving documents mention that in the spring of 1713, a nocturnal earthquake caused many fatalities with damage to villages throughout Bhutan (92° – 93°E [Ambraseys and Jackson, 2003]). Were this a great earthquake, these authors speculate that it may have been responsible for damage to temples reported at 95°E near Sadiya at an imprecisely known year circa 1714. The implied widespread shaking in 1714 would require a significant earthquake. It seems to be the case since

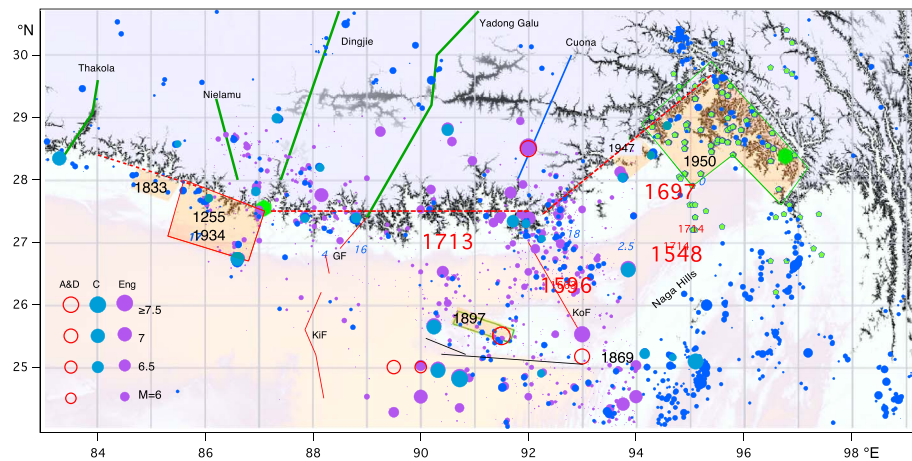


Figure 5. Recent seismicity (Eng=PDE and Engdahl and Villaseñor, [2002]), twentieth century (C=Centennial catalog), nineteenth century (A and D=Ambraseys and Douglas, 2004), and dates and approximate locations of historical earthquakes with unknown magnitude from Iyengar et al. [1999]. KiF = Kishinganj Fault, KoF = Kopili fault zone, and GF = Gish fault. The large green hexagons are the main shock locations for the 1934 and 1950 earthquakes, and the small green hexagons are the aftershocks of the 1950 earthquake [Chen and Molnar, 1977]. The elevations greater than 3.5 km north of the locking line (red dashed line) are grey. The numbers near the MFT indicate the paleoseismic trench estimates of paleoseismic slip. The green lines are rift zones. The blue line is a converging rift zone.

radiocarbon dating of alluvial terrace offsets along the MFT in Bhutan suggests an approximate displacement of ~ 10 m for the 1713 earthquake [Berthet et al., 2014]. Rajendran and Rajendran [2011] argue that the survival of the Medieval *Sil Háko* bridge (26.3°N, 91.65°E) until its destruction in the 1897 earthquake suggests that no great earthquake occurred in the preceding eight centuries. This ruined 42 m wide bridge lies midway between the 1897 rupture and the Himalayan frontal fault in Bhutan and might be expected to experience similar intensities (MSK VII+ [Ambraseys and Bilham, 2003]) during great Himalayan ruptures. However, in 1851, prior to its destruction, Hannay [1852] deduced from irregular markings on its 2 m long deck monoliths that part of the bridge had been reassembled imperfectly. He attributed the timing of its misalignment to repairs after a thirteenth century invasion, and this interpretation has been adopted by subsequent historians. It is possible however that imperfect reassembly followed damage sustained in a more recent earthquake penultimate to the 1897 catastrophe, possibly that postulated to have occurred after 1570 ± 80 A.D. [Berthet et al., 2014] from paleoseismic evidence, which may correspond to the historical 1713/1714 earthquake described above.

Paleoseismic trenching reveals that parts of the Himalayan décollement in east central Nepal slipped in 1255 and 1934 [Sapkota et al., 2013]. The mean slip in 1934, if the cumulative intervening slip deficit were released seismically, would have been ≈ 12 m, assuming the persistence of recent GPS convergence rates of 18 mm/yr during this time interval (Table 2). This is in satisfactory agreement with its 9 m slip calculated from its observed teleseismic moment release, equivalent to $M_w = 8.4$ with 5° dip [Molnar and Qidong, 1984], assuming a $130 \text{ km} \times 100 \text{ km}$ rupture area. In easternmost Nepal, paleoseismic trenching reveals lesser slip (4 m) with no clear indication of the observed dates for earthquakes [Nakata et al., 1998; Upreti et al., 2007]. Offsets in trench excavations of the Main Frontal Thrust, east and west of Bhutan (16 m and 18 m, respectively), have been interpreted as contiguous rupture in ≈ 1100 A.D. [Kumar et al., 2010]. The continuity of rupture however is equivocal, since the date of a synchronous earthquake affecting these two sites could postdate materials interred as late as the fourteenth century [cf. Kumar et al., 2010, Figure 12]. These investigators have also excavated trenches on the Arunachal Pradesh segment to the east of Bhutan: at 91°E, with possible slip circa 1100 of 2.5 m, and at 95°E with large, but undefined slip and a post 66 A.D. date [Jayangondaperumal et al., 2011]. A search for liquefaction features predating the 1950 $M_w = 8.5$ earthquake in the same region suggests an event that may have occurred after 1370 A.D., tentatively ascribed to historical earthquakes in 1548 and 1697 by Reddy et al. [2008].

Historical and paleoseismic data are thus presently equivocal concerning the existence or location of great ruptures in the past millennium (Figure 5). The 1548 and 1697 earthquakes reported from the north and south sides of the Brahmaputra Valley at $\approx 94.5^\circ\text{E}$ were associated with long-aftershock sequences and liquefaction

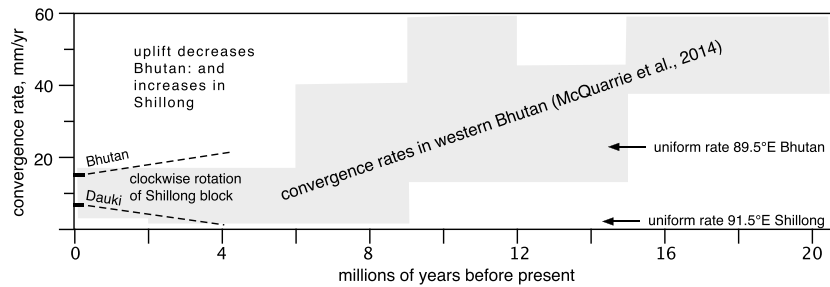


Figure 6. Present-day GPS (bold lines) and inferred north-south convergence rates across Bhutan and the Dauki fault assuming $\approx 45^\circ$ N dip [Ferguson et al., 2013]. Uplift rates increased on the Shillong Plateau 8–14 Ma [Clark and Bilham, 2008] at about the time that inferred rates decreased in Bhutan (grey area indicates the range of inferred shortening rate changes inferred by McQuarrie et al. [2014]), consistent with the decrease in exhumation 4–5 Ma noted by Coutand et al. [2014]. The dashed lines with equal and opposite slopes suggest that the initiation of clockwise rotation of the Shillong block relative to the Indian Plate 5 Ma may be responsible for both a decrease in convergence velocity in Bhutan and a simultaneous increase in velocity in Shillong. The slopes of the dashed lines are conjectural.

phenomena suggestive of $M > 7.5$ earthquakes. Based on the evidence that the last earthquake to rupture the Himalaya between 88°E and 90°E occurred after 1570 ± 80 A.D. and possibly as recently as 1713, the slip deficit would now be 5–8 m, similar to that inferred from alluvial terraces offsets. If this slip deficit was to be released near Bhutan by a $90 \text{ km} \times 150 \text{ km}$ Himalayan décollement earthquake, its magnitude would be equal or greater than $M_w = 8.2$, assuming complete release of elastic energy coseismically. Based on suggested structural segmentation between Sikkim and Arunachal Pradesh, Drukpa et al. [2012] develop several M_{max} scenarios for great earthquakes in the eastern Himalayan with magnitudes in the range $8.2 < M_w < 8.9$.

3. Discussion

The Bhutan Himalaya lacks a prominent foredeep or a corresponding flexural bulge as is found south of the central Himalaya [Jordan and Watts, 2005]. A mechanical explanation for this is that the southern edge of the Shillong block is elevated by stresses arising from thrust faulting, and that the block is tilted northward at approximately $2\text{--}4^\circ$ (Figure 4c) as indicated by a 1–2 km increase in depth of the Moho between the northern edge of the plateau and the Himalaya [Mitra et al., 2005] and by the concordance of summits of inselbergs exposed in the Brahmaputra Valley. The plateau corresponds to a significant high gravity, indicating that it is not in isostatic equilibrium, and south of the Dauki fault, the front edge of the Shillong Plateau is thrust over, and into, the great thickness of sediments in Bangladesh that overlie oceanic crust there [Chen and Molnar, 1990; Steckler et al., 2008].

An unexpected result alluded to in an earlier section of this article is the $\approx 13^\circ$ dip to the Dauki fault required to reconcile geological estimates for the vertical rise of the Shillong Plateau [Biswas et al., 2007; Clark and Bilham, 2008] with present-day rates of convergence between the Shillong block and the Indian Plate described here. A dip closer to $\approx 45^\circ$ has been assumed in previous studies [e.g., Bilham and England, 2001]; however, this is not constrained by focal mechanism solutions, geodesy, microseismicity, or by active seismic source studies. A steep dip to the fault is consistent with the gravity gradient [Verma and Mukhopadhyay, 1977], with receiver function interpretations [Biswas et al., 2007] and from considerations of structural faulting elsewhere [Scholz, 2002]. The surface Dauki fault may in fact be vertical, absorbing the partitioned dextral component of slip derived in the GPS models, whereas the thrust component is concealed beneath the influx of recent sediments in Bangladesh [Ferguson et al., 2013].

One way to escape the conclusion that the Dauki fault has shallow dip is to invoke a recent increase in the convergence rate between the Shillong Plateau and the Indian Plate. If a 45° dip to the fault prevails, the present-day rate would need to have more than doubled recently compared to its mean rate in the past 8–14 Myr for the mean exhumation rate to be reconciled with the recent GPS convergence rate. We hypothesize that this can most easily be explained by a recent 3–8 mm/yr decrease in the rate of convergence across the Bhutan Himalaya. Intriguingly, detailed studies of variable uplift rates in Bhutan are consistent with a slowing in the inferred convergence rate between the Shillong block and the southern Tibet [McQuarrie et al., 2014; Coutand et al., 2014]. In Figure 6 we illustrate synchronous slowing in west Bhutan convergence

and increasing convergence on the eastern end of the Dauki fault. The correspondence requires that the Shillong block fractured from the Indian Plate at some time in the past 4–5 Ma and that convergence rates >10 Ma on the Himalayan décollement in Bhutan were ≈ 5 mm/yr faster than at present, i.e., 20–23 mm/yr.

A consequence of this inferred recent N/S convergence rate change is that the present mean uplift rate of the Shillong Plateau at 91°E (assuming 45°N dip to the Dauki fault) is approximately 5 mm/yr. This fast rate of rise is not manifest in the past several years of GPS data, leveling data, since it occurs only during incremental faulting (e.g., ≈ 10 m in the 1897 earthquake). Depending on the geometry of the transition of convergent creep beneath the Shillong Plateau to the Indian Plate in northern Bangladesh, we anticipate that present-day elastic uplift signal of 0.3–2 mm/yr may prevail locally.

The northern limits of the Shillong and Assam blocks beneath the Himalaya and southern Tibet are unknown, but their rotation may account for the observed oblique widening of the rift zones of the SE Tibetan Plateau [Gan *et al.*, 2007] (Figure 1). The sinistral shear associated with relative motion of the Shillong and Himalaya regions might also be responsible for the strike-slip focal mechanisms located below the MHT [Drukpa *et al.*, 2006]. In this case the partitioning would not be accommodated by a strike-slip fault located above the thrust fault but by shearing of the downgoing plate. The striking change in the style of continental collision that occurs east of the Kishenganj fault [Dasgupta and Nandy, 1982; Dasgupta *et al.*, 2000] coincides with the termination of continental flexure and its replacement by fragmented rotating blocks. Presumably, the presence of numerous trans-Himalayan structures, the absence of a prominent foredeep, the abrupt changes in the width of the Himalayan décollement, and the 20° clockwise change in strike of the easternmost 400 km of the Himalaya (Figure 1a) are also related independent motion of the shearing we describe.

4. Conclusions

GPS measurements reveal the clockwise rotation of two blocks beneath the Brahmaputra Valley about points a few hundred kilometers to the west of the Shillong Plateau. The trailing edges of these blocks are being overtaken by the southward approach of the Tibetan Plateau at rates slower than those in the central Himalaya (14 ± 2 mm/yr). Where sufficient data exist (western Bhutan), we find no evidence for creep on the Himalayan décollement south of the locking line; hence, we conclude that a seismic slip deficit exists along the eastern Himalaya that will eventually drive segments to rupture in great earthquakes. The locked décollement is narrowest near Sikkim (55–70 km), attains a width of approximately 100 km in eastern Bhutan, and widens to >110 km in Arunachal Pradesh, where it veers abruptly 20° counterclockwise from the small circle that defines most of the Himalaya. Our data provide weak constraints for convergence of 11.5 ± 1 mm/yr in Arunachal Pradesh. Numerical solutions here are influenced by GPS velocities at the end of this segment and provide no constraints on locking depth or position in the central Arunachal segment due to an absence of GPS constraints near 95°E .

The current slip deficit on the segments of the Himalayan décollement is unclear because of the ambiguous historical and paleoseismic record of great earthquakes in Bhutan and Assam in the past millennium. A worst case scenario suggests that the slip deficit in all the segments of the eastern arc could exceed 12 m, similar to the slip inferred in discrete events exhumed in paleoseismic trenches along the main Himalayan frontal thrust fault. A number of poorly documented earthquakes in the seventeenth and eighteenth centuries may have partly released this slip deficit. However, had an earthquake in 1713 completely released the slip deficit in Bhutan, it would now have established a slip deficit of 5.4 m, sufficient to fuel a $M_w = 8.2$ earthquake, assuming a 150×90 km² rupture zone.

The slip deficit, prevailing beneath the Naga Hills south of the Assam block, is not well determined by our data. Décollement ruptures presumably occur here, and it is possible that surviving accounts of the 1548 Sadiya earthquake may describe such an earthquake. Assuming a conservative convergence rate of 2 mm/yr, a slip deficit of ≈ 1 m may now prevail near Sadiya; however, our data are unable to determine whether creep processes occur beneath the Naga Hills.

The eastern Assam block rotates slightly faster than the Shillong block resulting in ≈ 3 mm/yr of dextral shear across a diffuse zone of seismicity at the Kopili fault zone. Several recent earthquakes have occurred on the Kopili fault, one beneath the Himalaya [Kayal *et al.*, 2010]. It is probable that two damaging historical earthquakes occurred on the southern Kopili fault in the seventeenth century. The two blocks evidently

extend northward a considerable distance beneath the Tibetan Plateau, and although their northern edges are not defined by the measurements presented here, the rotation poles of the two blocks are consistent with oblique opening of rift zones reported 200 km north of the Himalaya on the Tibetan Plateau [Zhang *et al.*, 2004; Gan *et al.*, 2007].

The southern edge of the Assam block collides with the Naga Hills at 1–3 mm/yr and descends beneath the Naga Hills on a décollement dipping to the south. The Assam block is thereby flexed by the combined loads of the Himalaya and the Naga Hills. In contrast, the Shillong block is thrust over oceanic crust beneath Bangladesh and is tilted gently northward, with vigorous deformation only along its southern edge. We deduce that late in the past 8 Myr, the rate of convergence across the Dauki fault has increased, and the rate of convergence across the Bhutan Himalaya has decreased, as a result of the initiation of clockwise rotation of the Shillong block.

Convergence rates increase eastward across the Dauki fault such that the Dapsi fault and Oldham fault share a convergence rate of 3–5 mm/yr and the easternmost Dauki fault develops a slip deficit at 8 mm/yr. The renewal time for great earthquakes in the western Shillong Plateau similar in magnitude to the 1897 earthquake must exceed 2000 years.

Acknowledgments

The Bhutan measurements were funded by the National Science Foundation EAR 0739081, by the French "Agence Nationale de la Recherche" (ANR-07-JCJC-0015), and by the CNES-TOSCA. We thank N. Feld and F. Blume for their contributions measuring the first two sets of GPS positions in Bhutan and Shillong. We thank the Director of the Geological Survey of India for the GPS data from the easternmost Brahmaputra Valley and György Hetényi for the valuable information on Bhutan. Data supporting this study (GPS velocities) are available in Table S1 in the supporting information.

References

- Ader, T., *et al.* (2012), Convergence rate across the Nepal Himalaya and interseismic coupling on the main Himalayan thrust: Implications for seismic hazard, *J. Geophys. Res.*, *117*, B044403, doi:10.1029/2011JB009071.
- Ambraseys, N., and D. Jackson (2003), A note on early earthquakes in northern India and southern Tibet, *Curr. Sci.*, *84*, 570–582.
- Ambraseys, N. N., and J. Douglas (2004), Magnitude calibration of North Indian earthquakes, *Geophys. J. Int.*, *158*, 1–42, doi:10.1111/j.1365-246X.2004.02323.x.
- Ambraseys, N., and R. Bilham (2003), MSK isoseismal intensities evaluated for the 1897 Great Assam Earthquake, *Bull. Seismol. Soc. Am.*, *93*(2), 655–673.
- Angelier, J., and S. Baruah (2009), Seismotectonics of North East India: A stress analysis of focal mechanism solutions of earthquakes and its kinematic implications, *Geophys. J. Int.*, *178*, 303–326.
- Armijo, R., P. Tapponier, J. L. Mercier, and T.-L. Han (1986), Quaternary extension in southern Tibet: Field observations and tectonic implications, *J. Geophys. Res.*, *91*, 13,803–13,872, doi:10.1029/JB091iB14p13803.
- Banerjee, P., R. Bürgmann, B. Nagarajan, and E. Apel (2008), Intraplate deformation of the Indian subcontinent, *Geophys. Res. Lett.*, *35*, L18301, doi:10.1029/2008GL035468.
- Banerji, R. D. (1923), The Haihuyas of Tripuri and their monuments, Memoir 23, 152 pp. with 57 illustrations, Archaeological Survey of India, Calcutta.
- Bendick, R., and R. Bilham (2001), How perfect is the Himalayan Arc?, *Geology*, *29*, 791–794.
- Berthet, T., *et al.* (2013), Lateral uniformity of India Plate strength over central and eastern Nepal, *Geophys. J. Int.*, *195*(3), 1481–1493, doi:10.1093/gji/ggt357.
- Berthet, T., *et al.* (2014), Active tectonics of the eastern Himalaya: New constraints from the first tectonic geomorphology study in southern Bhutan, *Geology*, *42*(5), 427, doi:10.1130/G35162.1.
- Bilham, R., and P. England (2001), Plateau "pop-up" in the great 1897 Assam earthquake, *Nature*, *410*(6830), 806–809, doi:10.1038/35071057.
- Biswas, S., I. Coutand, D. Grujic, C. Hager, D. Stöckli, and B. Grasemann (2007), Exhumation and uplift of the Shillong plateau and its influence on the eastern Himalayas: New constraints from apatite and zircon (U-Th-[Sm])/He and apatite fission track analyses, *Tectonics*, *26*, TC6013, doi:10.1029/2007TC002125.
- Bollinger, L., J. P. Avouac, R. Cattin, and M. R. Pandey (2004), Stress buildup in the Himalaya, *J. Geophys. Res.*, *109*, B11405, doi:10.1029/2003JB002911.
- Burgess, W. P., A. Yin, C. S. Dubey, Z.-K. Sehn, and T. K. Kelty (2012), Holocene shortening across the main frontal thrust zone in the eastern Himalaya, *Earth Planet. Sci. Lett.*, *357*, 152–167.
- Chen, Q., J. T. Freymueller, Z. Yang, C. Xu, W. Jiang, Q. Wang, and J. Liu (2004), Spatially variable extension in southern Tibet based on GPS measurements, *J. Geophys. Res.*, *109*, B09401, doi:10.1029/2002JB002350.
- Chen, W.-P., and P. Molnar (1977), Seismic moments of major earthquakes and the average rate of slip in Central Asia, *J. Geophys. Res.*, *82*, 2945–2969, doi:10.1029/JB082i020p02945.
- Chen, W.-P., and P. Molnar (1990), Source parameters of earthquakes and intraplate deformation beneath the Shillong Plateau and the Northern Indoburman Ranges, *J. Geophys. Res.*, *95*(B8), 12,527–12,552, doi:10.1029/JB095iB08p12527.
- Choudhury, R. D. (1985), Archaeology of the Brahmaputra Valley of Assam: Pre-Ahom period, Agim-Kala Prakashanm Delhi, 271 pp.
- Clark, M. K., and R. Bilham (2008), Miocene rise of the Shillong Plateau and the beginning of the end for the Eastern Himalaya, *Earth Planet. Sci. Lett.*, *269*(3), 337–351, doi:10.1016/j.epsl.2008.01.045.
- Coutand, I., D. M. Whipp Jr., D. Grujic, M. Bernet, M. G. Fellin, B. Bookhagen, K. R. Landry, S. K. Ghalley, and C. Duncan (2014), Geometry and kinematics of the Main Himalayan Thrust and Neogene crustal exhumation in the Bhutanese Himalaya derived from inversion of multithermochronologic data, *J. Geophys. Res. Solid Earth*, *119*, 1446–1481, doi:10.1002/2013JB010891.
- Dahlen, F. A. (1990), Critical taper model of fold-and-thrust belts and accretionary wedges, *Annu. Rev. Earth Planet. Sci.*, *18*, 55–99.
- Dasgupta, S., and D. R. Nandy (1982), Seismicity and tectonics of the Menghalaya Plateau, Northwestern India, VII Symp. on Earthquake Engineering, Univ. of Roorkee, Nov 10–12, vol. 1, 19–24.
- Dasgupta, S., M. Mukhopadhyay, and D. R. Nandy (1987), Active transverse features in the central portion of the Himalaya, *Tectonophysics*, *136*, 255–264.
- Dasgupta, S., *et al.* (2000), *Seismotectonic Atlas of India and Its Environs*, edited by P. L. Narula, S. K. Acharyya, and J. Banerjee, 87 pp., Geol. Surv. India, Calcutta, India.

- Drukpa, D., A. A. Velasco, and D. I. Doser (2006), Seismicity in the Kingdom of Bhutan (1937–2003): Evidence for crustal transcurrent deformation, *J. Geophys. Res.*, *111*, B06301, doi:10.1029/2004JB00.
- Drukpa, D., P. Pelgay, A. Bhattacharya, P. Vernant, W. Szeliga, and R. Bilham (2012), GPS constraints on Indo-Asian convergence in the Bhutan Himalaya: Segmentation and potential for a 8.2 M_w <math>< 8.8</math> earthquake. HKT meeting, Kathmandu, Nepal Dec 2012, *J. Nepal Geol. Soc.*, *45*(Special Issue), 43–44.
- Engdahl, E. R., and A. Villaseñor (2002), Global seismicity: 1900–1999, in *International Handbook of Earthquake and Engineering Seismology, Part A*, edited by W. H. K. Lee et al., chap. 41, pp. 665–690, Academic Press, San Diego, Calif.
- Ferguson, E. K., L. Seeber, M. S. Steckler, S. H. Akhter, D. Mondal, and A. Lenhart (2013), The Dauki Thrust Fault and the Shillong Anticline: An incipient plate boundary in NE India? AGU Fall Meeting T51F-2665. [Available at <http://fallmeeting.agu.org/2012/eposters/eposter/t51f-2665/>]
- Gahalaut, V., and K. Gahalaut (2007), Burma Plate motion, *J. Geophys. Res.*, *112*, B10402, doi:10.1029/2007JB004928.
- Gahalaut, V. K., et al. (2013), Aseismic plate boundary in the Indo-Burmese wedge, northwest Sunda Arc, *Geology*, *41*(2), 235–238, doi:10.1130/G33771.1.
- Gait, E. A. (1906), *A History of Assam*, 385 pp., Thacker Spink & Co., Calcutta, India.
- Gan, W., P. Zhang, Z.-Y. Shen, Z. Niu, M. Wang, Y. Wan, D. Zhou, and J. Cheng (2007), Present-day crustal motion within the Tibetan Plateau inferred from GPS measurements, *J. Geophys. Res.*, *112*, B08416, doi:10.1029/2005JB004120.
- Godard, V., J. Lavé, J. Carcaillet, R. Cattin, D. Bourles, and J. Zhu (2010), Spatial distribution of denudation in Eastern Tibet and regressive erosion of plateau margins, *Tectonophysics*, *491*(1), 253–274, doi:10.1016/j.tecto.2009.10.026.
- Hammer, P., et al. (2013), Flexure of the India plate underneath the Bhutan Himalaya, *Geophys. Res. Lett.*, *40*, 4225–4230, doi:10.1002/grl.50793.
- Hannay, S. T. (1852), Brief notice of the Sil Háko or stone bridge in Zilla Kamrup, *J. Roy. As. Soc. Bengal*, *1851*(IV), 291–294.
- Herring, T. A., R. W. King, and S. C. McClusky (2009), *GAMIT reference manual, Release 10.3*, Massachusetts Institute of Technology, Cambridge.
- Hough, S., and R. Bilham (2008), Site response of the Ganges Basin inferred from re-evaluated macroseismic observations from the M8.1 Shillong 1897, M7.8 Kangra 1905 and 1934 Nepal M8.1 earthquakes, *J. Earth Syst. Sci.*, *117*(S2), 773–782.
- Ismail-Zadeh, A., J.-L. Le Mouél, A. Soloviev, P. Tapponnier, and I. Vorovieva (2007), Numerical modeling of crustal block-and-fault dynamics, earthquakes and slip rates in the Tibet-Himalayan region, *Earth Planet. Sci. Lett.*, *258*, 465–485.
- Iyengar, R. N., D. Sharma, and J. M. Siddiqui (1999), Earthquake history of India in Medieval Times, *Indian J. Hist. Sci.*, *34*(3), 181–237.
- Jade, S., et al. (2007), Estimates of interseismic deformation in Northeast India from GPS measurements, *Earth Planet. Sci. Lett.*, *263*(3–4), 221–234, doi:10.1016/j.epsl.2007.08.031.
- Jayangondaperumal, R., S. G. Wesnousky, and B. K. Choudhuri (2011), Near-surface expression of early to late Holocene displacement along the northeastern Himalayan frontal thrust at Marbang Korong Creek, Arunachal Pradesh, India, *Bull. Seismol. Soc. Am.*, *101*(6), 3060–3064.
- Jordan, T. A., and A. B. Watts (2005), Gravity anomalies, flexure and the elastic thickness structure of the India-Eurasia collisional system, *Earth Planet. Sci. Lett.*, *236*, 732–750.
- Karakhanyan, A., et al. (2013), GPS constraints on continental deformation in the Armenian region and Lesser Caucasus, *Tectonophysics*, *592*(C), 39–45, doi:10.1016/j.tecto.2013.02.002.
- Kayal, J. R., S. S. Arefiev, S. Barua, D. Hazarika, N. Gogoi, A. Kumar, S. N. Chowdhury, and S. Kalita (2006), Shillong plateau earthquakes in northeast India region: Complex tectonic model, *Curr. Sci.*, *91*(1), 109–113.
- Kayal, J. R., S. S. Arefiev, S. Baruah, R. Tatevossian, N. Gogoi, M. Anajam, J. L. Gautam, D. Hazarika, and D. Borah (2010), The 2009 Bhutan and Assam felt earthquakes (M_w 6.3 and 5.1) at the Kopili fault in the northeast Himalaya region, *Geomatics, Nat. Hazards Risk*, *1*(3), 273–281, doi:10.1080/19475705.2010.486561.
- Kumar, S., S. G. Wesnousky, T. K. Rockwell, R. W. Briggs, V. C. Thakur, and R. Jayangondaperumal (2006), Palaeoseismic evidence of great surface rupture earthquakes along the Indian Himalaya, *J. Geophys. Res.*, *111*, B03304, doi:10.1029/2004JB003309.
- Meade, B. J. (2007), Present-day kinematics at the India-Asia collision zone, *Geology*, *35*, 81–84, doi:10.1130/G22924A.1.
- Kumar, S., S. G. Wesnousky, R. Jayangondaperumal, T. Nakata, Y. Kumahara, and V. Singh (2010), Paleoseismological evidence of surface faulting along the northeastern Himalayan front, India: Timing, size, and spatial extent of great earthquakes, *J. Geophys. Res.*, *115*, B12422, doi:10.1029/2009JB006789.
- Maurin, T., F. Masson, C. Rangin, U. T. Min, and P. Collard (2010), First global positioning system results in northern Myanmar: Constant and localized slip rate along the Sagaing fault, *Geology*, *38*(7), 591–594, doi:10.1130/G30872.1.
- McCaffrey, R. (2002), *Crustal Block Rotations and Plate Coupling, Plate Boundary Zones: AGU Geodynamics Series*, edited by S. Stein and J. T. Freymueller, pp. 101–122, AGU, Washington, D. C.
- McQuarrie, N., T. Tobgay, S. P. Long, P. W. Reiners, and M. A. Cosca (2014), Variable exhumation rates and variable displacement rates: Documenting recent slowing of Himalayan shortening in western Bhutan, *Earth Planet. Sci. Lett.*, *386*(2014), 161–174.
- Meade, B. (2007), Present day kinematics at the India-Asia collision zone, *Geology*, *35*(1), 81–84, doi:10.1130/G22924A.1.
- Mitra, S., K. Priestley, A. K. Bhattacharyya, and V. K. Gaur (2005), Crustal structure and earthquake focal depths beneath northeastern India and southern Tibet, *Geophys. J. Int.*, *160*, 227–248, doi:10.1111/j.1365-246X.2004.02470.x.
- Molnar, P., and D. Qidong (1984), Faulting associated with large earthquakes and the average rate of deformation in central and eastern Asia, *J. Geophys. Res.*, *89*, 6203–6227, doi:10.1029/JB089iB07p06203.
- Morino, M., A. S. M. Maksud Kamal, D. Muslim, R. M. E. Ali, M. A. Kamal, M. Z. Rahman, and F. Kaneko (2011), Seismic event of the Dauki Fault in 16th century confirmed by trench investigation at Gabrakhari Village, Haluaghat, Mymensingh, Bangladesh, *J. Asian Earth Sci.*, *42*(3), 492–498.
- Mullick, M., F. Riguzzi, and D. Mukhopadhyay (2009), Estimates of motion and strain rates across active faults in the frontal part of eastern Himalayas in North Bengal from GPS measurements, *Terra Nova*, *21*, 410–415, doi:10.1111/j.1365-3121.2009.00898.x.
- Nakata, T. (1972), Geomorphical history and crustal movements of the foothills of the Himalayas, *Sci. Rep. Tohoku Univ.*, *Ser. 7*, 22, 39–177.
- Nakata, T. (1989), Active faults of the Himalaya of India and Nepal, in *Tectonics of the Western Himalayas*, *Geol. Soc. of Am. Spec. Pap.* 232, edited by L. L. Malinconico Jr. and R. J. Lillie, pp. 243–264, Geol. Soc. Am., Boulder, Colo.
- Nakata, T., et al. (1998), First successful paleoseismic trench study on active faults in the Himalaya, *Eos Trans. AGU*, *79*(45), Fall Meet Suppl., Abstract S22A-18.
- Ni, J., and M. Barazangi (1984), Seismotectonics of the Himalayan Collision Zone: Geometry of the underthrusting Indian Plate beneath the Himalaya, *J. Geophys. Res.*, *89*(B2), 1147–1163, doi:10.1029/JB089iB02p01147.
- Okada, Y. (1985), Surface deformation due to shear and tensile faults in a half-space, *Bull. Seismol. Soc. Am.*, *75*(4), 1135–1154.
- Oldham, R. D. (1899), Report on the great earthquake of June 12, 1897, *Mem. Geol. Surv. India*, *29*, 1–379.
- Rajendran, K., and C. P. Rajendran (2011), Revisiting some significant earthquake sources in the Himalaya: Perspectives on past seismicity, *Tectonophysics*, *504*, 75–88.
- Reddy, D. V., P. Nagabhushanam, D. Kumar, B. S. Sukhija, P. J. Thomas, A. K. Pandey, R. N. Sahoo, G. V. Ravi Prasad, and K. Datta (2008), The great 1950 Assam Earthquake revisited: Field evidences of liquefaction and search for paleoseismic events, *Tectonophysics*, *474*(3), 463–472, doi:10.1016/j.tecto.2009.04.024.

- Sapkota, S. N., L. Bollinger, Y. Klinger, P. Tapponier, Y. Gaudemer, and D. Tiwari (2013), Primary surface ruptures of the great Himalayan earthquakes in 1934 and 1255, *Nat. Geosci.*, *6*, 71–76.
- Schiffman, C., B. S. Bali, W. Szeliga, and R. Bilham (2013), Seismic slip deficit in the Kashmir Himalaya from GPS observations, *Geophys. Res. Lett.*, *40*, 5642–5645, doi:10.1002/2013GL057700.
- Scholz, C. H. (2002), *The Mechanics of Earthquakes and Faulting*, 2nd ed., Cambridge Univ. Press, Cambridge.
- Seeber, L., and V. Gornitz (1983), River profiles along the Himalayan arc as indicators of active tectonics, *Tectonophysics*, *92*, 335–467.
- Shen, Z.-K., J. Lü, M. Wang, and R. Burgmann (2005), Contemporary crustal deformation around the southeast borderland of the Tibetan Plateau, *J. Geophys. Res.*, *110*, B11409, doi:10.1029/2004JB003421.
- Steckler, M., S. H. Akhter, and L. Seeber (2008), Collision of the Ganges-Brahmaputra Delta with the Burma Arc, *Earth Planet. Sci. Lett.*, *273*, 367–378.
- Thatcher, W. (2007), Microplate model for the present-day deformation of Tibe, *J. Geophys. Res.*, *112*, B01401, doi:10.1029/2005JB004244.
- Upreti, B. N., Y. Kumahara, and T. Nakata (2007), Paleoseismological study in the Nepal Himalaya—Present status, Proceedings of the Korea-Nepal Joint symposium on slope stability and landslides April 1, 2007, p. 1–9.
- Verma, R. K., and M. Mukhopadhyay (1977), An analysis of gravity field in northeastern India, *Tectonophysics*, *42*, 283–317.
- White, J. C. (1909), *Sikhim and Bhutan: Twenty One Years on the North East Frontier, 1887 1908*, 331 pp., Longmans Green and Co.: Edward Arnold, London.
- Zhang, P. Z., Z. Shen, M. Wang, W. J. Gan, R. Burgmann, and P. Molnar (2004), Continuous deformation of the Tibetan Plateau from global positioning system data, *Geology*, *32*(9), 809–812, doi:10.1130/g20554.1.